Transmembrane Voltage Induced by Applied Electric Fields

59

Tadej Kotnik

Abstract

An exposure of a biological cell to an electric field results in the induced transmembrane voltage (ITV) proportional to the strength of the electric field and superimposed onto the resting transmembrane voltage for the duration of the exposure. The ITV can have a range of effects from modification of the activity of voltage-gated channels to membrane electroporation, and accurate knowledge of spatial distribution and time course of the ITV is important both for the studies of these phenomena and for effectiveness of their applications. Unlike the resting component of the transmembrane voltage, the induced component varies with position on the membrane, it depends on the shape of the cell and its orientation with respect to the electric field, and in dense cell suspensions and tissues also on the volume fraction occupied by the cells. Inducement of the ITV is a process characterized by a time constant, which amounts to tenths of a microsecond under physiological conditions. As a consequence, the time course of the ITV lags the time course of the electric field that induces it, and for exposures to alternating fields with frequencies above 1 MHz or to pulses with durations below 1 μs, the amplitude of the ITV induced by the field of a given amplitude starts to decrease with further increase of the field frequency or with further decrease of the pulse duration. With field frequencies approaching the GHz range or with pulse durations in the ns range, this attenuation of the ITV comes to a halt, and the voltages induced on the organelle membranes inside the cell can reach the same order of magnitude as the voltage induced by the same field on the plasma membrane, and under certain conditions even exceed it. After the description of methods for analytical derivation and numerical computation of the ITV, the main techniques for experimental determination of ITV are also outlined.

T. Kotnik (✉)
Faculty of Electrical Engineering, University of Ljubljana, Ljubljana, Slovenia
e-mail: tadej.kotnik@fe.uni-lj.si

D. Miklavčič (ed.), *Handbook of Electroporation*,
DOI 10.1007/978-3-319-32886-7_8

Keywords

Induced transmembrane voltage • Electric pulses • Plasma membrane • Organelle membranes • Schwan's equation • Finite-elements method • Potentiometric dyes • Electroporation

Contents

Introduction

From the electrical point of view, the cell can roughly be described as an electrolyte (the cytoplasm) surrounded by an electrically insulating shell (the plasma membrane), and the natural surroundings of a cell typically also resemble an electrolyte quite closely. Under such conditions, when a cell is exposed to an electric field, the field locally concentrates within the membrane, which thus shields the cytoplasm from the exposure. For this reason, the internal structure of the cell is unimportant, except with rapidly time-varying electric fields, where, as discussed in section "High Field Frequencies and Very Short Pulses," the transient exposure of the intracellular structures to the field must also be taken into account for proper analysis, and both the membrane and its surroundings have to be treated as materials with a both nonzero electric conductivity and a nonzero dielectric permittivity.

The concentration of the electric field inside the membrane results in a considerable electric potential difference across the membrane, termed the induced transmembrane voltage (ITV), which superimposes onto the resting transmembrane voltage (RTV) resulting from the imbalances between intracellular and extracellular ion concentrations and amounting under physiological conditions to tens of millivolts. After the electric field ceases, so does the ITV, and only the RTV remains on the membrane. Modification of transmembrane voltage through ITV can affect the functioning of voltage-gated membrane channels, thus initiating action potentials and stimulating excitable cells (Bedlack et al. 1994; Cheng et al. 1999; Burnett et al. 2003), and when sufficiently large it can also lead to either reversible or irreversible electroporation of the cells' plasma membrane (Neumann et al. 1999),

with the porated membrane regions closely correlated with the regions of the highest absolute value of transmembrane voltage (Kotnik et al. 2010). It should be noted that not only does the ITV affect electroporation, but once the membrane is electroporated, its significantly increased electric conductivity also affects the ITV, which decreases from the value induced immediately before the onset of electroporation, and generally the more intense the electroporation, the larger is this decrease.

Using Ψ to denote electric potential, transmembrane voltage is the difference between the potentials at the inner and the outer membrane surface, Ψ_{int} and Ψ_{ext}, and in physiology RTV is always defined and measured as

$$\Delta\Psi_m = \Psi_{int} - \Psi_{ext} \quad , \tag{1}$$

so that a negative value reflects a lower electric potential of the cytosol with respect to the cell exterior. For superposition of the ITV onto the RTV to be applicable also formally, one should adhere to Eq. 1 also when characterizing the ITV, and this chapter does so; thus, the RTV can be superimposed to the ITV by simple mathematical addition to yield the total transmembrane voltage, and this chapter henceforth only deals with the induced transmembrane voltage, using the acronym ITV in the text and the notation $\Delta\Psi_m$ in the formulae.

From the geometrical point of view, the cell can be characterized as a geometric body (the cytoplasm) surrounded by a shell of uniform thickness (the membrane). For suspended cells, the simplest model of the cell is a homogeneous sphere surrounded by a spherical shell. For augmented generality, the sphere can be replaced by a cylinder (e.g., as a model of the axon of a neuron), a spheroid (e.g., an oblate spheroid as a model of an erythrocyte or a prolate spheroid as a model of a bacillus), or an ellipsoid, but with spheroids and ellipsoids the realistic requirement of uniform membrane thickness complicates the geometrical description of the shell: if its outer surface is characterized as a spheroid or an ellipsoid, its inner surface lacks a simple geometrical characterization and vice versa. The steady-state ITV on the plasma membrane of such cells can, however, still be determined analytically.

Spheres, spheroids, and ellipsoids are reasonable models for most suspended cells but not for those in tissues. No simple geometrical body can model a typical cell in a tissue, where furthermore each cell generally differs in its shape from the rest. With cells of irregular shape and/or close to each other, the ITV cannot be derived analytically and cannot be formulated as an elementary mathematical function. This deprives us of some of the insight available from explicit expressions, but with spatial and temporal discretization on modern computers, the ITV induced on an irregular cell of interest can still be estimated rather accurately, provided that the three-dimensional shape of this cell is determined with sufficient accuracy. Numerical computation is generally also required to assess the ITV after the cell is electroporated, as this increases the electric conductivity of the membrane significantly (invalidating its treatment as an insulating shell) and moreover nonuniformly.

Section "Analytical Derivation and Numerical Computation of ITV" provides a more detailed description of methods for analytical derivation and numerical

computation of ITV, while section "Experimental Determination of ITV" outlines the main techniques for experimental determination of ITV.

Analytical Derivation and Numerical Computation of ITV

Spherical Cells

For an exposure to a homogeneous electric field, the ITV is determined by solving Laplace's equation. Although biological cells are not perfect spheres, in the simplest theoretical treatment they are considered as such, and for an approximation, the plasma membrane can be treated as nonconductive. Under these assumptions, the process of solving Laplace's equation with appropriate boundary conditions (Kotnik and Pucihar 2010) yields a description of the ITV often referred to as the steady-state Schwan's equation (Pauly and Schwan 1959),

$$\Delta\Psi_{\mathrm{m}} = \frac{3}{2} E R \cos\theta \ , \tag{2}$$

where E is the strength of the electric field in the region where the cell is situated (i.e., the local electric field), R is the cell radius, and θ is the angle measured from the center of the cell with respect to the direction of the field. The ITV on the membrane of a spherical cell is thus proportional to the applied electric field and to the cell radius and has extremal values at the points where the field is perpendicular to the membrane, i.e., at $\theta = 0^\circ$ and $\theta = 180^\circ$ (the "poles" of the cell), while in-between these poles it varies proportionally to the cosine of θ (see Fig. 1, dashed).

The value of the ITV given by Eq. 2 is typically established several μs after the onset of the electric field. With exposures to a DC field lasting hundreds of microseconds or more, this formula can safely be applied to yield the maximal, steady-state value of the ITV. To describe its transient behavior during the initial microseconds, one uses the first-order Schwan's equation (Pauly and Schwan 1959),

$$\Delta\Psi_{\mathrm{m}} = \frac{3}{2} E R \cos\theta \ \left(1 - \exp(-t/\tau_{\mathrm{m}})\right) \ , \tag{3}$$

where τ_{m} is the time constant of membrane charging,

$$\tau_{\mathrm{m}} = \frac{R\,\varepsilon_{\mathrm{m}}}{2d\dfrac{\sigma_{\mathrm{i}}\sigma_{\mathrm{e}}}{\sigma_{\mathrm{i}} + 2\sigma_{\mathrm{e}}} + R\sigma_{\mathrm{m}}} \tag{4}$$

with σ_{i}, σ_{m}, and σ_{e} the conductivities of the cytoplasm, cell membrane, and extracellular medium, respectively, ε_{m} the dielectric permittivity of the membrane, d the membrane thickness, and R again the cell radius.

In certain experiments *in vitro*, where artificial extracellular media with conductivities substantially lower than physiological are used, the factor 3/2 in Eqs. 2 and 3

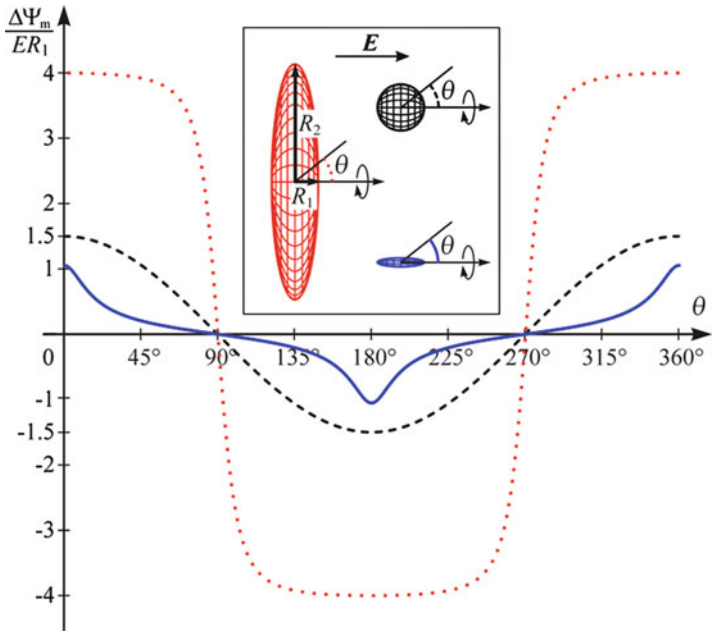

Fig. 1 Normalized steady-state ITV as a function of the polar angle θ for spheroidal cells with the axis of rotational symmetry aligned with the direction of the field. *Solid*: a prolate spheroidal cell with $R_2 = 0.2 \times R_1$. Dashed: a spherical cell, $R_2 = R_1 = R$. *Dotted*: an oblate spheroidal cell with $R_2 = 5 \times R_1$

decreases in value, as described in detail in (Kotnik et al. 1997). But generally, Eqs. 3 and 4 are applicable to exposures to sinusoidal (AC) electric fields with frequencies below 1 MHz and to electric pulses longer than 1 μs.

To determine the ITV induced by even higher field frequencies or even shorter pulses, the dielectric permittivities of the electrolytes on both sides of the membrane also have to be accounted for. This leads to a further generalization of Eqs. 3 and 4 to the second-order Schwan equation (Grosse and Schwan 1992; Kotnik et al. 1998; Kotnik and Miklavčič 2000a), and the results it yields will be outlined in subsection "High Field Frequencies and Very Short Pulses."

Nonspherical Geometrically Regular Cells

Another direction of generalization is to assume a cell shape more general than that of a sphere. The most straightforward generalization is to a spheroid (a geometrical body obtained by rotating an ellipse around one of its radii, so that one of its orthogonal projections is a sphere and the other two are the same ellipse) and further to an ellipsoid (a geometrical body in which each of its three orthogonal projections is a different ellipse). To obtain the analogues of Schwan's equation for such cells,

one solves Laplace's equation in spheroidal and ellipsoidal coordinates, respectively (Kotnik and Miklavčič 2000b; Gimsa and Wachner 2001; Valič et al. 2003). Besides the fact that this solution is by itself somewhat more intricate than the one in spherical coordinates, the generalization of the shape invokes two additional complications outlined in the next two paragraphs.

A description of a cell is geometrically realistic if the thickness of its membrane is uniform. This is the case if the membrane represents the space between two concentric spheres but not with two confocal spheroids or ellipsoids. As a result, the thickness of the membrane modeled in spheroidal or ellipsoidal coordinates is necessarily nonuniform. By solving Laplace's equation in these coordinates, one thus obtains the spatial distribution of the electric potential in a nonrealistic setting. However, for cells surrounded by a physiological medium and with nonporated membranes, the electric conductivity of the membrane can be neglected (i.e., the membrane is treated as an insulator), and the steady-state ITV obtained in this manner is still realistic, as the electric potential everywhere inside the cytoplasm is constant, and the geometry of the inner surface of the membrane does not affect the potential distribution outside the cell, which is the same as if the cell would be a homogeneous nonconductive body of the same shape; a rigorous discussion of the validity of this approach is given in (Kotnik and Miklavčič 2000b). Figure 1 shows the ITV for a spherical cell, as described by the steady-state Schwan's equation, and for two spheroidal cells with their axis of rotational symmetry aligned with the direction of the field, as described by the expressions analogous to the Schwan's equation that are valid for such cell shapes (Kotnik and Pucihar 2010).

For nonspherical cells, it is generally more revealing to express the ITV as a function of the arc length along the membrane rather than as a function of the angle θ on the membrane (for a sphere, the two quantities are directly proportional). For uniformity, the normalized version of the arc length is used, denoted by p and increasing from 0 to 1 equidistantly along the arc of the membrane. This is depicted in Fig. 2 for the three cells for which the ITV as a function of θ is shown in Fig. 1, and in this chapter all subsequent plots of the ITV for nonspherical cells will be presented in this manner.

The second complication of generalizing the cell shape from a sphere to a spheroid or an ellipsoid is that the ITV now also depends on the orientation of the cell with respect to the electric field. To deal with this, one decomposes the field vector into the components parallel to the axes of the spheroid or the ellipsoid and writes the ITV as a corresponding linear combination of the ITV for each of the three coaxial orientations (Gimsa and Wachner 2001; Valič et al. 2003). Figures 3 and 4 show the effect of rotation of two different spheroids with respect to the direction of the field.

Irregularly Shaped Cells

For an irregularly shaped cell, the ITV cannot be expressed as an elementary mathematical function, since for such a geometry Laplace's equation is not solvable analytically, but using modern computers and the finite-elements method

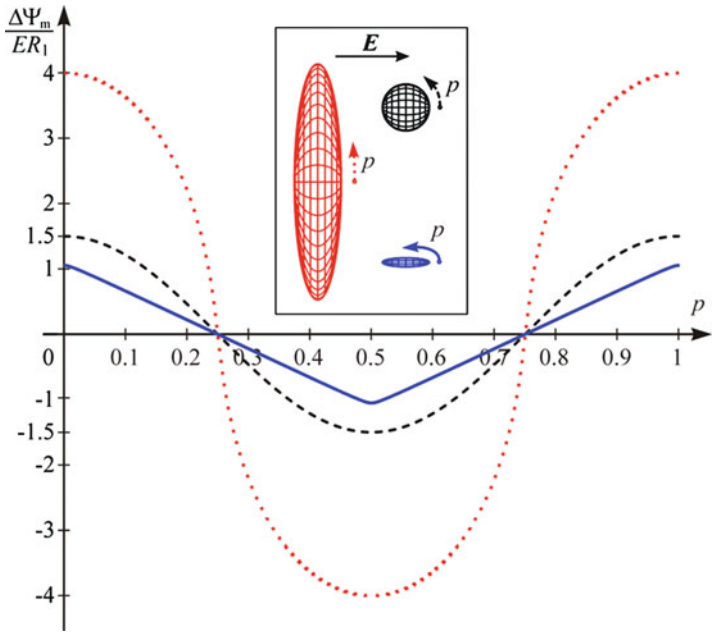

Fig. 2 Normalized steady-state ITV as a function of the normalized arc length p for spheroidal cells with the axis of rotational symmetry aligned with the direction of the field. *Solid*: a prolate spheroidal cell with $R_2 = 0.2 \times R_1$. *Dashed*: a spherical cell, $R_2 = R_1 = R$. *Dotted*: an oblate spheroidal cell with $R_2 = 5 \times R_1$

implemented in software packages such as COMSOL Multiphysics, the ITV on a given irregular cell can be determined numerically (Pucihar et al. 2006; Pucihar et al. 2009a). With a sufficiently accurately determined three-dimensional shape of the cell and with sufficiently fine spatial and temporal resolution, the ITV obtained in this manner is quite accurate, but it should be kept in mind that the set of ITV values so obtained over the membrane of the cell under consideration is only applicable to this cell, i.e., for the cell of the particular shape and size for which the three-dimensional shape has been determined and on which the ITV has been computed. Figure 5 shows examples of two cells growing in a Petri dish and the ITV computed on their membranes.

Cells in Dense Suspensions and Tissues

In natural situations the cells are rarely isolated, and when they are sufficiently close to each other, the mutual distortion of the field caused by their proximity becomes nonnegligible. Often, the cells are also in direct contact, forming two-dimensional (monolayers attached to the bottom of a dish) or three-dimensional (tissues) structures, and they can even be electrically interconnected.

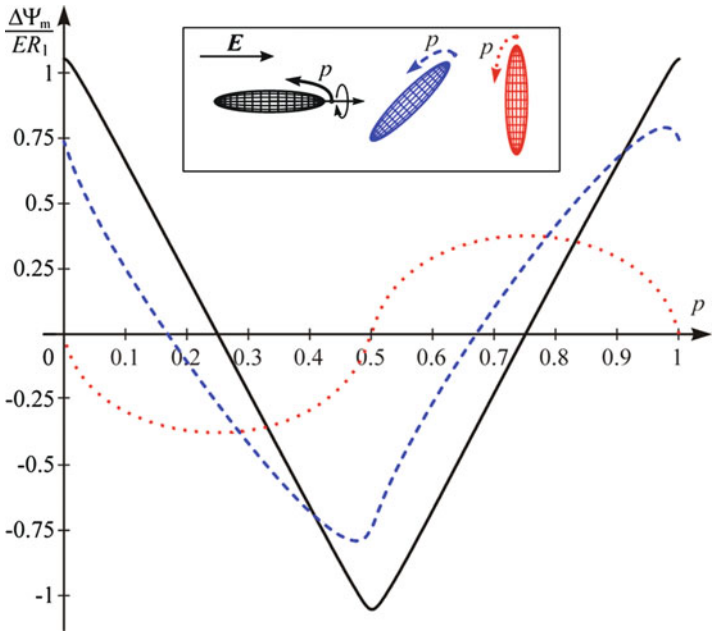

Fig. 3 Normalized steady-state ITV as a function of p for a prolate spheroidal cell with $R_2 = 0.2 \times R_1$. *Solid*: axis of rotational symmetry (*ARS*) aligned with the field. *Dashed*: ARS at 45° with respect to the field. *Dotted*: ARS perpendicular to the field

In dilute cell suspensions, the distance between the cells is much larger than the cells themselves, and the local field outside each cell is almost unaffected by the presence of other cells. Thus, for cells representing less than ∼1% of the suspension volume (for spherical cells with radii of ∼10 μm, this corresponds to up to ∼2 million cells/ml), the deviation of the actual ITV from the one predicted by Schwan's equation is negligible. However, as the volume fraction occupied by the cells gets larger, the distortion of the local field around each cell by the presence of other cells in the vicinity becomes more pronounced, and the ITV starts to differ noticeably from the prediction yielded by Schwan's equation (Fig. 6), and an accurate estimation of the ITV must be assessed either numerically of by analytical approximations (Susil et al. 1998; Pavlin et al. 2002). Regardless of the volume fraction the cells occupy, suspended cells float rather freely, so their arrangement is on average rather uniform, resembling a face-centered cubic lattice, which is thus the most appropriate choice for models of dense cell suspensions (Pavlin et al. 2002; Pucihar et al. 2007).

For even larger volume fractions of the cells, the electrical properties of the suspension start to approach that of a tissue but only to a certain extent; the arrangement of cells in tissues does not necessarily resemble a face-centered lattice, since cells differ from each other, form specific structures (e.g., layers), and can also be directly electrically coupled (e.g., through gap junctions).

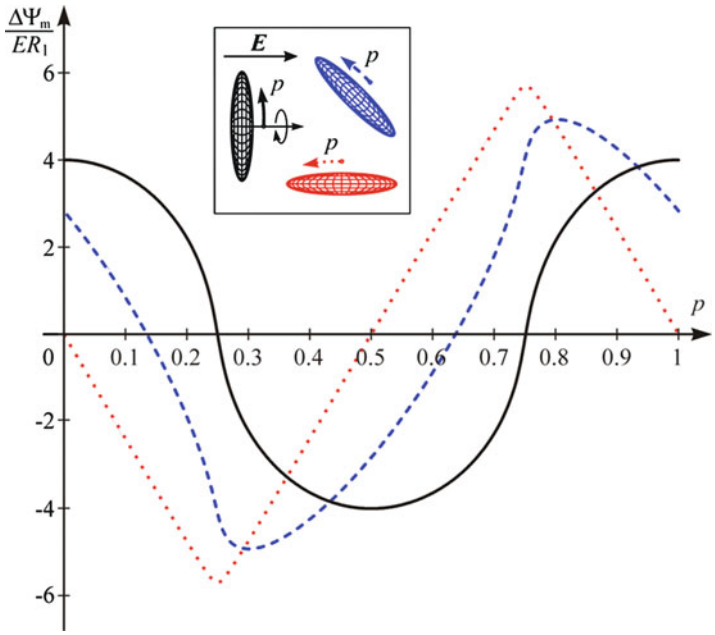

Fig. 4 Normalized steady-state ITV as a function of p for an oblate spheroidal cell with $R_2 = 5 \times R_1$. *Solid*: axis of rotational symmetry (*ARS*) aligned with the field. *Dashed*: ARS at 45° with respect to the field. *Dotted*: ARS perpendicular to the field

High Field Frequencies and Very Short Pulses

The time constant of membrane charging (τ_m) given by Eq. 4 implies that there is a lag between the time courses of the external field and the ITV induced by this field. As mentioned above, τ_m (and thus the lag) is in tenths of a microsecond under physiological conditions but can be longer when cells are suspended in a medium with electric conductivity substantially below physiological levels. For alternating (AC) fields with the oscillation period much longer than τ_m, as well as for rectangular pulses much longer than τ_m, the effect of this lag on the amplitude of the ITV is negligible. However, for AC fields with the period shorter than τ_m, as well as for pulses shorter than τ_m, the amplitude of the ITV gets attenuated by the lag, and with further increase in field frequency or decrease in pulse duration, the amplitude of the ITV induced by the field of a given amplitude starts to decrease. Figure 7 shows this attenuation for a spherical cell; the low-frequencies plateau of the amplitude and its intermediate-frequencies decrease are both described by the first-order Schwan's equation, but the high-frequencies plateau is only described by the second-order version of this equation, for derivation of which all electric conductivities and dielectric permittivities are taken into account (Kotnik et al. 1998; Kotnik and Miklavčič 2000a).

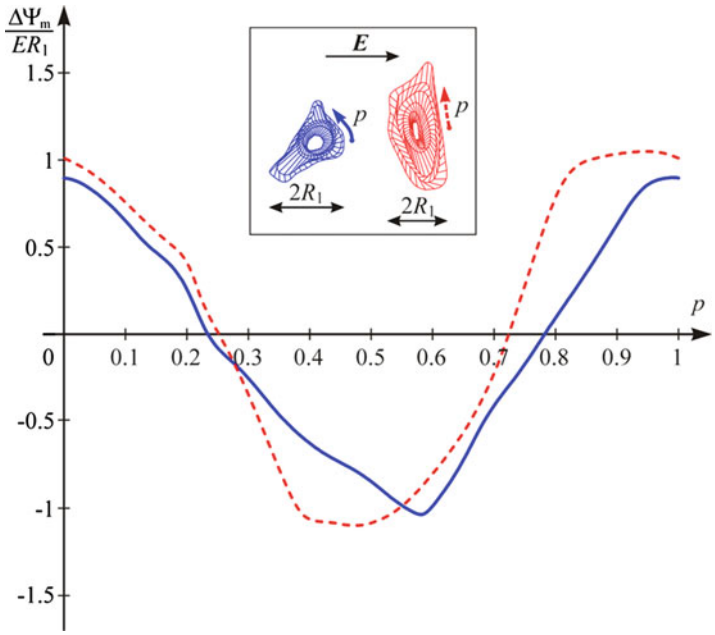

Fig. 5 Normalized steady-state ITV as a function of p for two irregularly shaped cells growing on the flat surface of a Petri dish, with the *inset* showing the top view of the cells

With field frequencies approaching the GHz range or with pulse durations in the ns range, this attenuation of the ITV comes to a halt, and the voltages induced on the organelle membranes inside the cell are of the same order of magnitude as the voltage induced by the same field on the plasma membrane. In certain circumstances, particularly if the organelle interior is electrically more conductive than the cytosol or if the organelle membrane has a lower dielectric permittivity than the cell membrane, the ITV on the membrane of such an organelle can temporarily even exceed the ITV on the plasma membrane (Kotnik and Miklavčič 2006). In principle, this could provide a theoretical explanation for reports that very short and intense electric pulses (tens of ns, millions of V/m) can also induce electroporation of organelle membranes (Schoenbach et al. 2001; Beebe et al. 2003; Tekle et al. 2005; Batista Napotnik et al. 2016).

Experimental Determination of ITV

An alternative to the analytical and numerical methods for determining the ITV are the experimental techniques – measurements of the ITV with microelectrodes and with potentiometric fluorescent dyes. Microelectrodes were used in pioneering measurements of the action potential propagation, first conventionally (Ling and Gerard 1949) and later as patch-clamp electrodes (Neher and Sakmann 1976),

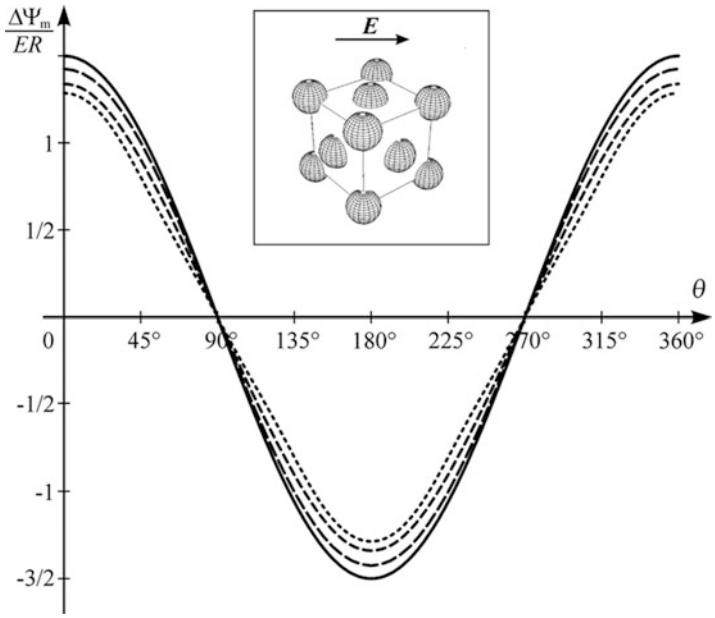

Fig. 6 Normalized steady-state ITV as a function of p for spherical cells in suspensions of various densities (intercellular distances). *Solid*: The analytical result for a single cell as given by Eq. 2. *Dashed*: numerical results for cells arranged in a face-centered cubic lattice and occupying (with decreasing dash size) 10%, 30%, and 50% of the total suspension volume

preferred for their simple use and high temporal resolution. However, the invasive nature of measurements and low spatial resolution are considerable shortcomings of this approach. Furthermore, the physical presence of the conductive electrodes during the measurement affects the distribution of the electric field around them and thus also the ITV. In contrast, measurements by means of potentiometric dyes are noninvasive, offer much higher spatial resolution, and do not distort the electric field and consequently the ITV. In addition, a potentiometric measurement can be performed simultaneously on a number of cells. For these reasons, the potentiometric dyes have during the last decades become the predominant method in experimental studies and measurements of the ITV, and the remainder of this chapter focuses exclusively on this approach.

Potentiometric Dyes

Based on their response mechanism, potentiometric dyes are divided into two classes: (i) slow potentiometric dyes that are translocated across the membrane by an electrophoretic mechanism, which is accompanied by a fluorescence change and (ii) fast potentiometric dyes that incorporate into the membrane, with energy levels

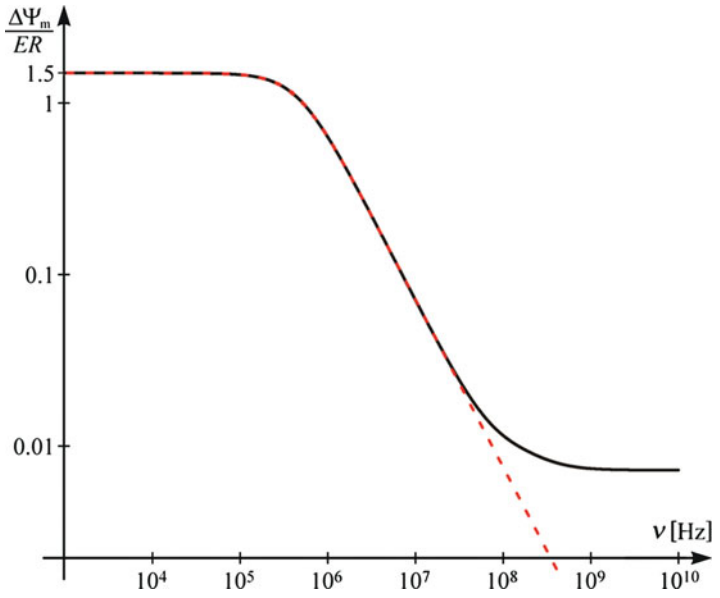

Fig. 7 The amplitude of normalized steady-state ITV as a function of the frequency of the AC field. The *dashed curve* shows the first-order and the *solid curve* the second-order Schwan's equation. Note that both axes are logarithmic

of their electrons and consequently their fluorescence properties dependent on transmembrane voltage.

Electric pulses used in electrophysiological and electroporation-based applications usually have durations in the range of microseconds to milliseconds. To measure the ITV induced by such pulses, fast potentiometric dyes have to be used. These respond to changes in the ITV within microseconds or less, which makes them suitable even for measurements of the transient effects. Slow dyes, on the other hand, need several seconds to respond to a change in the transmembrane voltage, and while some of them, particularly rhodamine and several carbocyanines, are efficient in the measurements of the RTV, their tardiness makes them largely useless for analysis of the ITV.

One of the most widely used fast potentiometric dyes is di-8-ANEPPS (di-8-butylamino-naphthyl-ethylene-pyridinium-propyl-sulfonate), developed by Leslie Loew and colleagues at the University of Connecticut (Gross et al. 1986; Loew 1992). This dye is nonfluorescent in water but becomes strongly fluorescent when incorporated into the lipid bilayer of the cell membrane, thereby making the membrane highly visible. This enables the construction of spatial numerical models of cells from a set of cross-section fluorescence images (Pucihar et al. 2006), and thus provides a possibility to compute the ITV on the same cells on which an experiment is carried out.

The fluorescence intensity of di-8-ANEPPS varies proportionally to the change of the ITV; the response is linear for voltages ranging from −280 to +250 mV (Lojewska et al. 1989; Cheng et al. 1999). Relatively small changes in fluorescence of the dye, uneven membrane staining, and dye internalization make di-8-ANEPPS less suitable for measurements of the resting membrane voltage, although such efforts were also reported (Zhang et al. 1998). It is, however, well suited for measuring larger changes in membrane voltage, such as the onset of the ITV in nonexcitable cells exposed to external electric fields (Gross et al. 1986; Montana et al. 1989) or action potentials in excitable cells (Bedlack et al. 1994; Cheng et al. 1999). In addition, di-8-ANEPPS allows for determination of the ITV by ratiometric measurements of fluorescence excitation (Montana et al. 1989) or emission (Knisley et al. 2000), which increases the sensitivity of the response.

Image Acquisition and Data Processing

As the sensitivity of fast potentiometric dyes to the changes of the ITV is low (typically, a change by 100 mV results in the change of fluorescence intensity by 2–12%), the fluorescence changes are hardly discernible by the naked eye but become apparent with appropriate image processing and analysis.

This procedure is performed in several steps (Pucihar et al. 2009b). First, a pair of images is acquired: the control image (immediately before the exposure to the electric field) and the exposure image (during the delivery of the electric field pulse); to get a more reliable measurement, a sequence of pulses can be applied, with both the control and the exposure image acquired for each pulse. Second, the background fluorescence is subtracted from both images. Third, the region of interest corresponding to the membrane is determined for the cell under investigation, and the fluorescence intensities along this region in the control and pulse image are measured. Fourth, for each pulse, the control data are subtracted from the pulse data, and the result divided by the control data to obtain the relative fluorescence changes; if a sequence of pulses is applied, the values of relative fluorescence changes determined for each pulse can be averaged. Finally, the relative fluorescence changes are translated into ITV using the di-8-ANEPPS calibration curve; a rough estimation of this curve can be obtained from the literature, but for higher accuracy, it must be measured for each particular setup, as shown in Fig. 8. Calibration is performed with either (i) valinomycin, a potassium ionophore, and a set of different potassium concentrations in external medium (Montana et al. 1989; Pucihar et al. 2006, or (ii) patch clamp in voltage-clamp mode (Zhang et al. 1998). For a graphical description of the results, the ITV can be plotted as a function of the relative arc length. A brief summary of the described process in given in Fig. 9, showing a cell stained with di-8-ANEPPS, the processed image reflecting the ITV, and the plot of the ITV along the cell membrane. To remove some of the noise inherent to potentiometric measurements, the ITV curve can be smoothed using a suitable filter (e.g., a moving average).

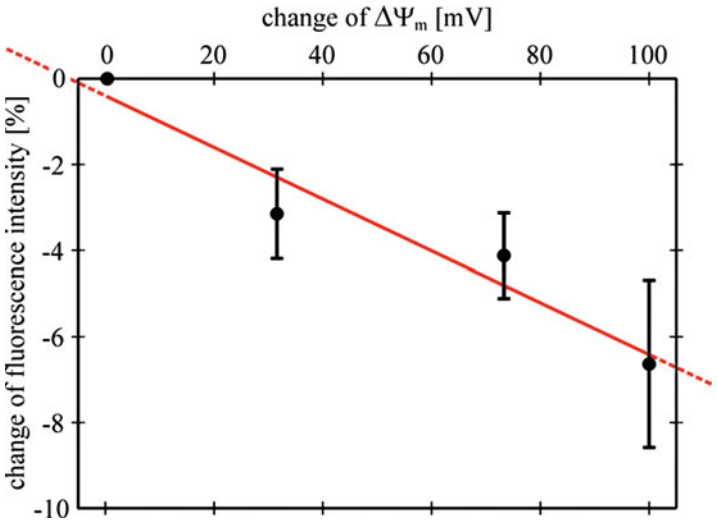

Fig. 8 An example of the experimental calibration curve for measurements of the ITV with di-8-ANEPPS

Conclusions

Knowledge and understanding of transmembrane voltage and the process of its inducement in cells exposed to electric fields are important in electrophysiology, and perhaps even more so in research of electroporation and development of electroporation-based technologies and treatments. As outlined in this chapter, inducement of the ITV is a process, and although for alternating electric fields with frequencies up to the kHz range and for electric pulses lasting tens of μs or longer, it can be approximated as instantaneous, for higher frequencies and shorter pulses the inducement's time course must also be taken into account for an accurate description of the ITV and its effects. In the context of electroporation, the key aspect is the close correlation between the ITV and the electroporation-mediated transport across the membrane: the membrane regions with the highest absolute value of the ITV are commonly also the ones where the transport proceeds the fastest. While the ITV induced by a given electric field can generally be predicted quite accurately by means of analytical or numerical calculation, a valuable experimental complement in determination of the ITV is found in fast potentiometric dyes that allow, with adequate sample preparation, dye fluorescence calibration, image acquisition, and data processing to determine the actual ITV and compare it to the calculated predictions.

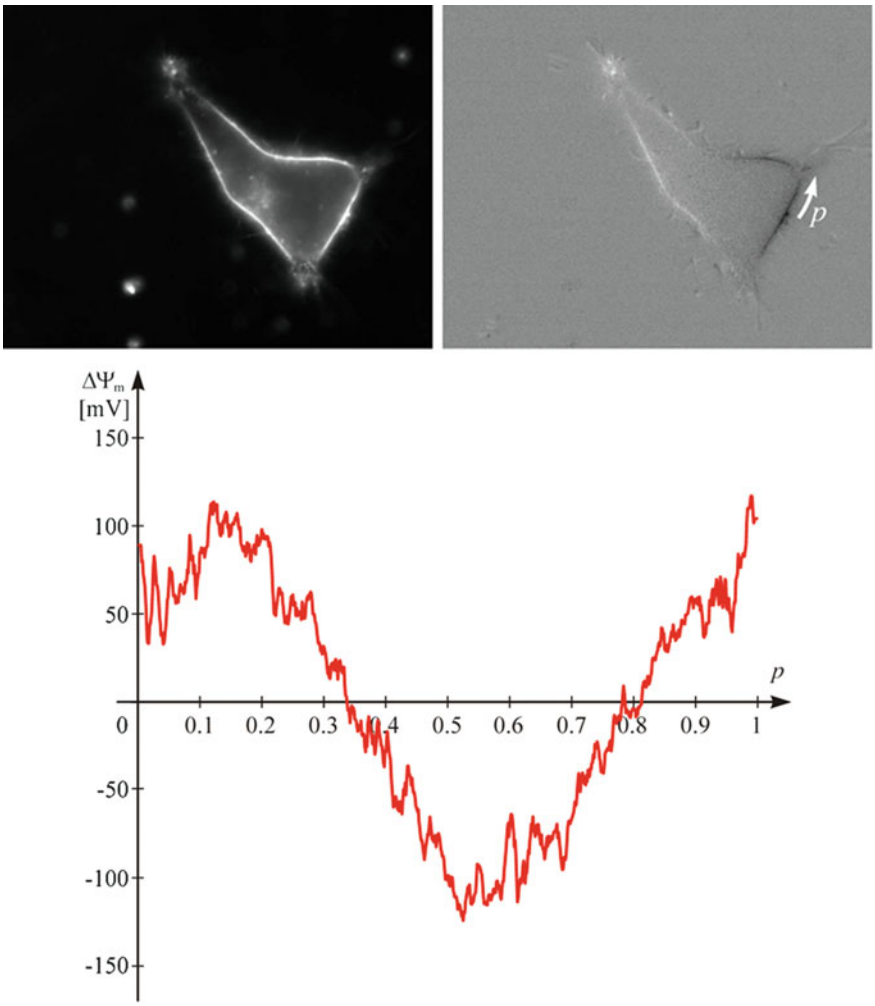

Fig. 9 Determination of the steady-state ITV with di-8-ANEPPS. *Top left*: Raw fluorescence image of a cell stained with di-8-ANEPPS. *Top right*: Processed image reflecting the ITV. *Bottom*: steady-state ITV as a function of p determined from the processed image using the calibration curve shown in Fig. 8

Acknowledgment This work was supported by the Slovenian Research Agency (Grant P2-0249) and conducted in the scope of the European Laboratory of Pulsed Electric Fields Applications (LEA EBAM) and within networking efforts of the COST Action TD1104 – European Network for Development of Electroporation-Based Technologies and Treatments (EP4Bio2Med).

Cross-References

- ▶ Critical Electric Field and Transmembrane Voltage for Lipid Pore Formation in Experiments
- ▶ Lipid Pores: Molecular and Continuum Models

References

Batista Napotnik T, Reberšek M, Vernier PT, Mali B, Miklavčič D (2016) Effects of high voltage nanosecond electric pulses on eukaryotic cells (in vitro): a systematic review. Bioelectrochemistry 110:1–12. doi:10.1016/j.bioelechem.2016.02.011

Bedlack RS, Wei M, Fox SH, Gross E, Loew LM (1994) Distinct electric potentials in soma and neurite membranes. Neuron 13:1187–1193. doi:10.1016/0896-6273(94)90056-6

Beebe SJ, Fox PM, Rec LJ, Willis EL, Schoenbach KH (2003) Nanosecond, high-intensity pulsed electric fields induce apoptosis in human cells. FASEB J 17:1493–1495. doi:10.1096/fj.02.0859fje

Burnett P, Robertson JK, Palmer JM, Ryan RR, Dubin AE, Zivin RA (2003) Fluorescence imaging of electrically stimulated cells. J Biomol Screen 8:660–667. doi:10.1177/1087057103258546

Cheng DK, Tung L, Sobie EA (1999) Nonuniform responses of transmembrane potential during electric field stimulation of single cardiac cells. Am J Physiol 277:H351–H362

Gimsa J, Wachner D (2001) Analytical description of the transmembrane voltage induced on arbitrarily oriented ellipsoidal and cylindrical cells. Biophys J 81:1888–1896. doi:10.1016/S0006-3495(01)75840-7

Gross D, Loew LM, Webb W (1986) Optical imaging of cell membrane potential changes induced by applied electric fields. Biophys J 50:339–348. doi:10.1016/S0006-3495(86)83467-1

Grosse C, Schwan HP (1992) Cellular membrane potentials induced by alternating fields. Biophys J 63:1632–1642. doi:10.1016/S0006-3495(92)81740-X

Knisley SB, Justice RK, Kong W, Johnson PL (2000) Ratiometry of transmembrane voltage-sensitive fluorescent dye emission in hearts. Am J Physiol Heart Circ Physiol 279:H1421–H1433

Kotnik T, Miklavčič D (2000a) Second-order model of membrane electric field induced by alternating external electric fields. IEEE Trans Biomed Eng 47:1074–1081. doi:10.1109/10.855935

Kotnik T, Miklavčič D (2000b) Analytical description of transmembrane voltage induced by electric fields on spheroidal cells. Biophys J 79:670–679. doi:10.1016/S0006-3495(00)76325-9

Kotnik T, Miklavčič D (2006) Theoretical evaluation of voltage inducement on internal membranes of biological cells exposed to electric fields. Biophys J 90:480–491. doi:10.1529/biophysj.105.070771

Kotnik T, Pucihar G (2010) Induced transmembrane voltage – theory, modeling, and experiments. In: Pakhomov AG, Miklavčič D, Markov MS (eds) Advanced electroporation techniques in biology and medicine. CRC Press, Boca Raton, pp 51–70

Kotnik T, Bobanović F, Miklavčič D (1997) Sensitivity of transmembrane voltage induced by applied electric fields – a theoretical analysis. Bioelectrochem Bioenerg 43:285–291. doi:10.1016/S0302-4598(97)00023-8

Kotnik T, Miklavčič D, Slivnik T (1998) Time course of transmembrane voltage induced by time-varying electric fields – a method for theoretical analysis and its application. Bioelectrochem Bioenerg 45:3–16. doi:10.1016/S0302-4598(97)00093-7

Kotnik T, Pucihar G, Miklavčič D (2010) Induced transmembrane voltage and its correlation with electroporation-mediated molecular transport. J Memb Biol 236:3–13. doi:10.1007/s00232-010-9279-9

Ling G, Gerard RW (1949) The normal membrane potential of frog sartorius fibers. J Cell Comp Physiol 34:383–396

Loew LM (1992) Voltage sensitive dyes: measurement of membrane potentials induced by DC and AC electric fields. Bioelectromagn Suppl 1:179–189. doi:10.1002/bem.2250130717

Lojewska Z, Farkas DL, Ehrenberg B, Loew LM (1989) Analysis of the effect of medium and membrane conductance on the amplitude and kinetics of membrane potentials induced by externally applied electric fields. Biophys J 56:121–128. doi:10.1016/S0006-3495(89)82657-8

Montana V, Farkas DL, Loew LM (1989) Dual-wavelength ratiometric fluorescence measurements of membrane-potential. Biochemistry 28:4536–4539. doi:10.1021/bi00437a003

Neher E, Sakmann B (1976) Single-channel currents recorded from membrane of denervated frog muscle fibres. Nature 260:779–802

Neumann E, Kakorin S, Toensing K (1999) Fundamentals of electroporative delivery of drugs and genes. Bioelectrochem Bioenerg 48:3–16. doi:10.1016/S0302-4598(99)00008-2

Pauly H, Schwan HP (1959) Über die Impedanz einer Suspension von kugelförmigen Teilchen mit einer Schale. Z Naturforsch 14B:125–131

Pavlin M, Pavšelj N, Miklavčič D (2002) Dependence of induced transmembrane potential on cell density, arrangement, and cell position inside a cell system. IEEE Trans Biomed Eng 49:605–612. doi:10.1109/TBME.2002.1001975

Pucihar G, Kotnik T, Valič B, Miklavčič D (2006) Numerical determination of the transmembrane voltage induced on irregularly shaped cells. Ann Biomed Eng 34:642–652. doi:10.1007/s10439-005-9076-2

Pucihar G, Kotnik T, Teissié J, Miklavčič D (2007) Electroporation of dense cell suspensions. Eur Biophys J 36:173–185. doi:10.1007/s00249-006-0115-1

Pucihar G, Miklavčič D, Kotnik T (2009a) A time-dependent numerical model of transmembrane voltage inducement and electroporation of irregularly shaped cells. IEEE T Biomed Eng 56:1491–1501. doi:10.1109/TBME.2009.2014244

Pucihar G, Kotnik T, Miklavčič D (2009b) Measuring the induced membrane voltage with di-8-ANEPPS. J Vis Exp 33:1659. doi:10.3791/1659

Schoenbach KH, Beebe SJ, Buescher ES (2001) Intracellular effect of ultrashort electrical pulses. Bioelectromagnetics 22:440–448. doi:10.1002/bem.71

Susil R, Šemrov D, Miklavčič D (1998) Electric field induced transmembrane potential depends on cell density and organization. Electro Magnetobiol 17:391–399

Tekle E, Oubrahim H, Dzekunov SM, Kolb JF, Schoenbach KH, Chock PB (2005) Selective field effects on intracellular vacuoles and vesicle membranes with nanosecond electric pulses. Biophys J 89:274–284. doi:10.1529/biophysj.104.054494

Valič B, Golzio M, Pavlin M, Schatz A, Faurie C, Gabriel B, Teissié J, Rols MP, Miklavčič D (2003) Effect of electric field induced transmembrane potential on spheroidal cells: theory and experiment. Eur Biophys J 32:519–528. doi:10.1007/s00249-003-0296-9

Zhang J, Davidson RM, Wei MD, Loew LM (1998) Membrane electric properties by combined patch clamp and fluorescence ratio imaging in single neurons. Biophys J 74:48–53. doi:10.1016/S0006-3495(98)77765-3